Materials Physics and Mechanics 47 (2021) 767-779
Research article

Received: October 13, 2021
Accepted: November 2, 2021

# LASER-DRIVEN METAL ALTERATION FOR GLUCOSE DETECTION SENSOR

**A. Kondrateva[1], V. Babyuk[1], D. Strekalovskaya[1], L. Filatov[1], P. Gabdullin[1]✉, O. Kvashenkina[1], Y. Prokopenko[1], A. Gruzdev[1], K. Petruhno[1], A. Kuznetsov[2]**

[1]Peter the Great St. Petersburg Polytechnic University, 29 Polytechnicheskaya str., 195251, St.-Petersburg, Russia

[2]Alferov St. Petersburg National Research Academic University, 8/1 Khlopina str., 194021, St.-Petersburg, Russia

✉ gabdullin_pg@spbstu.ru

**Abstract.** In this work, an experimental comparison of the laser-driven alteration of nickel, copper, and steel surface efficiency was carried out. The selection of the material most suitable for non-enzymatic measurement of the glucose amount in the medium was carried with respect to surface modification efficiency. The electrooxidative activity of the fabricated structures with a modified surface was investigated with respect to the glucose addition to a 0.1 M solution NaOH by potentiostatic method. The modified active NiO layer allows us the amperometric determination of glucose in the concentration range from 10 μM to 1.5 mM with sensitivity is higher than 10 μA/(mM·cm2) and the detection limit is not less than 5 μM. The proposed technology allows the manufacture of electrodes for non-enzymatic determination of glucose in alkaline solutions.

**Keywords:** laser alteration, surface, modification, glucose oxidation, sensor

***Acknowledgements.** The research is partially funded by the Ministry of Science and Higher Education of the Russian Federation as part of World-class Research Center program: Advanced Digital Technologies (contract No. 075-15-2020-934 dated 17.11.2020).*

**Citation:** Gabdullin P.G., Kondrateva A.S., Kvashenkina O.E., Babuk V.E., Strekalovskaya D.A., Filatov L.A. et al. Laser-driven metal alteration for glucose detection sensor // Materials Physics and Mechanics. 2021, V. 47. N. 5. P. 767-779. DOI: 10.18149/MPM.4752021_10.

## 1. Introduction

There is a sustained interest in glucose sensing currently. Glucose is one of the important metabolic intermediates whose reference level in human blood is 4.4-6.6 μM [1]. If the glucose level exceeds the above or is below the norm, it can lead to metabolic disorders (for example, provoke diabetes). Similarly, it is clinically important to control the substance in saliva and tears [2], sweat and urine [3], and others [4].

Generally, methods such as colorimetry, spectrophotometry, infrared spectroscopy, and electrochemical scanning are applied for monitoring glucose levels, and the choice is made taking into account the specifics of each of the techniques. Among the mentioned methods, electrochemical approach offers the advantages of high accuracy, facile scalability, and ease of analysis of the received measurement signal

http://dx.doi.org/10.18149/MPM.4752021_10

To count the glucose level in complex media, one can use enzymatic and more non-enzymatic electrochemical sensors that provide direct oxidation of glucose. Moreover, most modern sensor prototypes are ahead of the first in sensitivity and detection limit of the analyte [2,5]. It is only necessary to monitor the potential for the selectivity of the developed electrocatalysts (EC) with respect to glucose if the sensor is used in a very complex matrix solution [2]. A large number of transition metals (Pt, Ni, Au, Co, Ru, Cu, In) and alloys based on them (Au - Cu, Au - Ni, Pt - Pd, Ni - Cr, etc.) have been evaluated as a cathode material [1], transition metal oxides (NiO, $WO_3$, $RuO_2$, $MnO_2$, $Co_3O_4$, CuO, $TiO_2$, ZnO, $Fe_3O_4$) [1,6], as well as composite materials based on them [6,7]. But the sensitivity of the sensors is in the order of a few $\mu A/mM \cdot cm^2$ [8], which is still far from effective commercialization. To overcome the relatively low kinetics of the glucose electrooxidation reaction, strategies are being developed such as the fabrication of various nanostructures, an increase in the specific surface area, and doping.

Compared to bulk material, nanomaterials are much more responsive as a sensitive element of a sensor. For example, rods, piles, spheres, plates, layers, sheets, hollow and porous materials [9,10]. For this, a range of methods, techniques, and technological parameters were used [10,11]. Although these nanostructures usually exhibit high sensitivity, low detection limits and large linear measurement ranges for glucose concentration, their complex synthesis, low product yield, and high cost make such materials unattractive for industrial production [12]. The urgent task of developing a working electrode without complex and difficult to reproduce procedures [13].

Laser alteration techniques can offer an efficient, scalable manufacturing alternative to existing processing technologies, providing fast and controlled material processing to create functional micro- and nano-surfaces. The methods of laser-induced local modification make it possible to overcome many of the disadvantages of chemical synthesis and deposition processes, providing the possibility of direct creation of functional coatings: the laser beam locally processes the metal surface in a controlled environment. Thermal energy initiates both in-situ chemical oxidation (in an excess of oxygen) and texturing of the metal surface. Laser-induced metal alteration techniques are well understood and widely used as standard approaches to surface modification.

The aim of this work is to fabricate structures with a modified surface directly on electrodes for potential use in non-enzymatic measurement of glucose concentration. The proposed approach allows the one-stage synthesis of microstructures directly on the electrode surface in situ, providing reliable mechanical and electrical contact.

For this, the following tasks were set: selection of the oxide most suitable for use as a non-enzymatic measurement of the amount of glucose in the alkaly medium; investigation of the structure, composition, and morphology of the formed structures by methods of X-ray phase analysis, energy dispersive spectroscopy, optical microscopy; investigation of the electrooxidative activity in relation to the addition of 0.5 mM glucose to a 0.1 M sodium hydroxide solution by the potentiostatic method; investigation of the temporal stability of the electrochemical properties of fabricated sensitive structures.

## 2. Methods

Composites of NiO on Ni, CuO on Cu, and FeO on Steel surfaces for amperometric glucose detection were made by oxidation followed by laser-induced surface modification of metal foil in an ambient condition. The laser treatment was performed by using a low-power engraving laser Minimarker 2 with a wavelength of 1.064 µm. All parameters of laser radiation are set in the accompanying MaxiGraf software package. The output power of the laser system and the beam speed reach 20W and 5000 mm/s, respectively. The positioning accuracy of the laser beam is ± 0.1 µm.

SEM and EDX images were made by using the Mira 3 Tescan LMU with the EDX X-max 80 module, designed to obtain an image of the object's surface with high spatial resolution. The study of the sample structure was carried out using Raman spectroscopy, implemented on the basis of a LabRam HR800 Raman spectrometer. The measurements were carried out in the range 50-4000 $cm^{-1}$ at a pump power of 5.94 mW. The spectra were measured at several points of the samples under study and showed good agreement with each other, the figures will show one spectrum from each sample.

All electrochemical measurements were performed using electrochemical analyzer VersaStat 4 Princeton Applied Research. For cyclic voltammetry (CV) experiments back side of samples was passivated by epoxy resin, with 10×10 mm window. The rate of potential change was from 3 to 80 mV/s, 0.1 M NaOH was used as the electrolyte.

## 3. Results and Discussion

For the manufacture of electrodes, the method of laser-driven alteration of a metal surface was used. The key parameter for determining the degree of impact of laser radiation on a material is the energy flux incident on the surface per unit of time. This value can be determined indirectly from the results of exposure, however, to select the oxidation mode and repeatability of the experimental results, the energy flux was estimated from the first principles. In our case the estimation method is based on calculating the integral energy falling into the modified area, taking into account the energy of one pulse and the parameters of the focus point movement.

The energy per pulse for the modes used in the work is from $4\times10^{-5}$ to 0.2 mJ. To estimate the energy density, it is necessary to understand the nature of the beam path. The focal point moves across the surface in a manner similar to that of a scanning microscope (Fig. 1). The density of the grouping of the irradiated areas is controlled by several parameters – the speed of movement of the focusing point ($v$), line density ($N$), frequency ($F$).

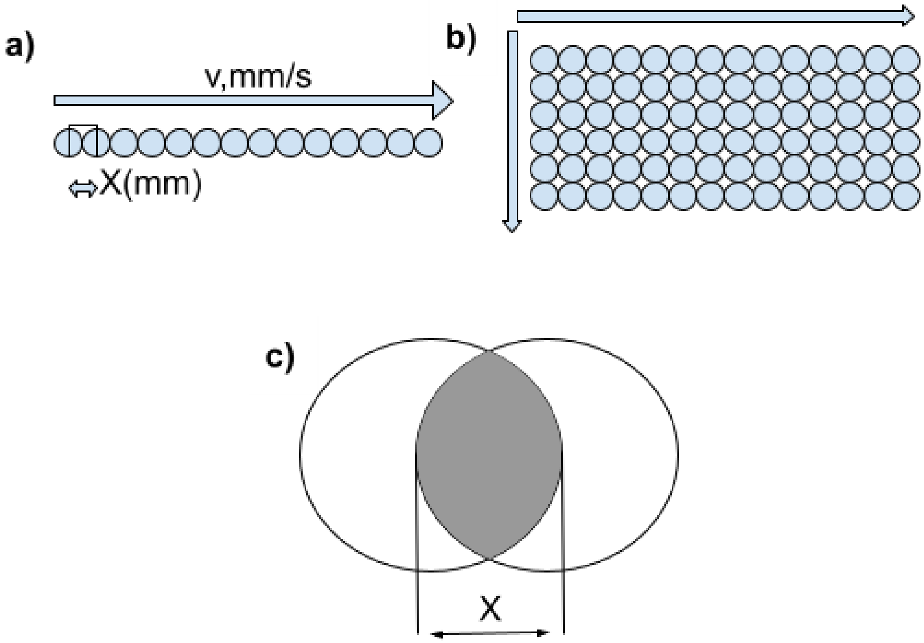

**Fig. 1.** Beam pass illustration

The distance between adjacent irradiated areas is calculated under the condition that the pulse repetition rate of the laser system and the speed of the beam are constant. The vertical line density is controlled by the $N$ – line density per mm. The program diameter of one "spot" is 10 μm. Thus, in order to obtain the result shown in Fig. 1 (b), it is necessary to select the parameters so that X to be 10 μm. This is possible, for example, at a frequency F of 50 kHz and a speed v of 500 mm/s, and a line density N of 100. In this operating mode with a duration of $\tau_{\max}$ is 200 ns and $P_{max}$ is 100%, $E_{eff}$ is 106 mJ/cm$^2$. Thus, it is possible to calculate the energy falling on 1 cm$^2$ of the area for all modes used in the work. The results of these calculations are presented in Table 1.

If the distance between the centers is less than the spot diameter, then overlap occurs. This overlap occurs in the vertical direction. The N was chosen equal to 200 lines per mm. And in one of the operating modes (the last line in Table 2), overlap also occurs horizontally.

Table 1. Summary for the irradiated area (per 1 cm$^2$)

| $F$, kHz | $\tau$, ns | $P$, % | $v$, mm/s | $N$, line/mm | $S$, cm$^2$ | $E_{Sum}$, J | $W$, W | $n$, piece |
|---|---|---|---|---|---|---|---|---|
| 50 | 100 | 10 | 500 | 200 | 0.45 | 20 | 0.50 | 2.00E+06 |
| 50 | 100 | 25 | 500 | 200 | 0.45 | 50 | 1.25 | 2.00E+06 |
| 50 | 100 | 50 | 500 | 200 | 0.45 | 100 | 2.50 | 2.00E+06 |
| 50 | 100 | 100 | 500 | 200 | 0.45 | 200 | 5.00 | 2.00E+06 |
| 50 | 20 | 50 | 500 | 200 | 0.45 | 20 | 0.50 | 2.00E+06 |
| 50 | 50 | 50 | 500 | 200 | 0.45 | 50 | 1.25 | 2.00E+06 |
| 50 | 100 | 50 | 500 | 200 | 0.45 | 100 | 2.50 | 2.00E+06 |
| 50 | 200 | 50 | 500 | 200 | 0.45 | 200 | 5.00 | 2.00E+06 |
| 10 | 100 | 50 | 500 | 200 | 0.09 | 20 | 0.50 | 4.00E+05 |
| 25 | 100 | 50 | 500 | 200 | 0.23 | 50 | 1.25 | 1.00E+06 |
| 50 | 100 | 50 | 500 | 200 | 0.45 | 100 | 2.50 | 2.00E+06 |
| 100 | 100 | 50 | 500 | 200 | 3.36 | 200 | 5.00 | 4.00E+06 |

It is also worth considering the surface reflectance. At the initial incidence of the beam, a significant part of the energy is reflected. To determine the part of the reflected energy, you can refer to the tabular data given in [14]. Thus, the magnitude of the values of the energy absorbed by the surface is of the order of tens joules.

Figure 2 shows the result of copper foil modification in the mode indicated in Table 1. It can be seen that laser-driven modification of copper (Fig. 2) leads to the formation of a structure in which it is difficult to see the lines of the laser beam. This is probably due to the high thermal conductivity of copper. Significant surface melting with the formation of a developed structure is observed. In addition, the image of the untreated part of the sample shows the presence of spherical particles, probably due to the inappropriate formation of metal droplets under the action of laser radiation.

Table 2. Results of energy dispersive surface studies. All results are in weight percent

| Point | O | Al | Cu |
|---|---|---|---|
| 1 | 1.28 | 0.00 | 98.72 |
| 2 | 2.60 | 0.41 | 96.99 |

EDX of the surface indicates (Table 2) that as a result of the laser-driven modification, the surface composition does not change significantly, except for the formation of spherical particles: it is composed of Cu 98.22 ± 0.05 in both regions, an increase in the amount of oxygen in the untreated region may be due to spherical particles representing is an oxide phase formed during the rapid oxidation of drops of molten copper. That is, when the surface is treated with a laser in air, the metal droplets knocked out by the laser beam are oxidized, which is confirmed by the results of Raman spectroscopy: the broadened peaks obtained are typical for copper and correlate well with [15]. There are no peaks in the range 200-900 cm$^{-1}$, which indicates the absence of noticeable oxide layers on the surface also.

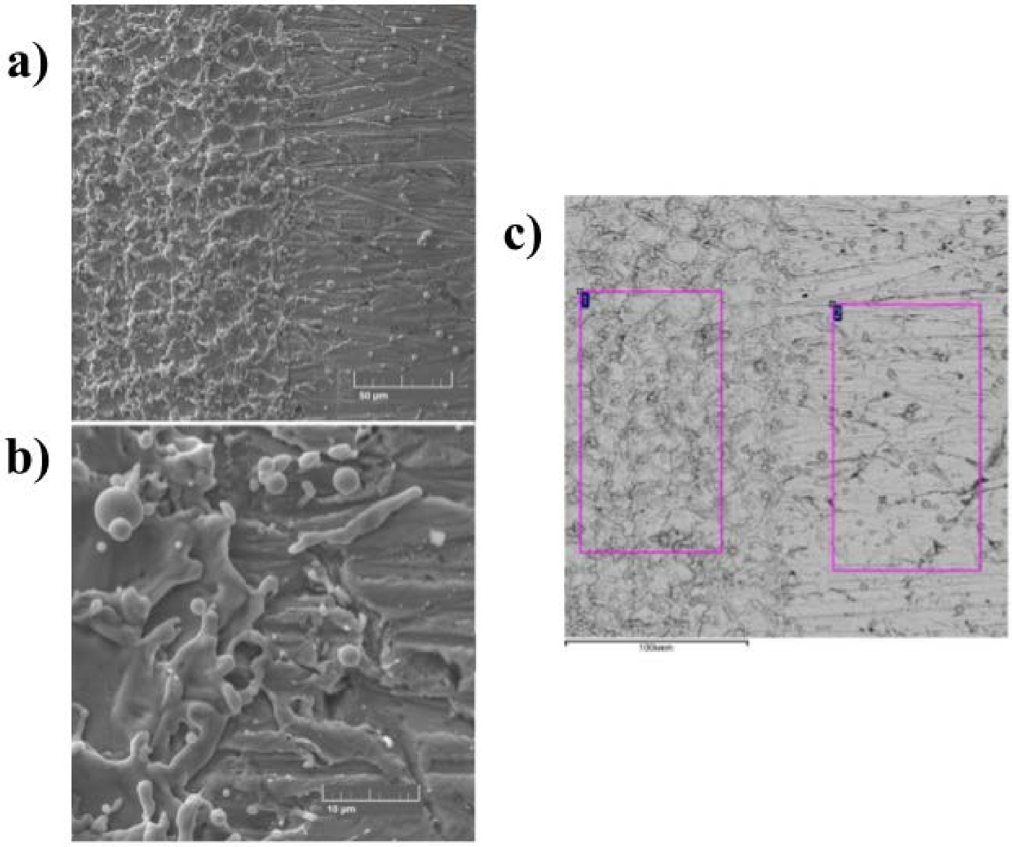

**Fig. 2.** (a, b) SEM images of the copper electrode surface at the border of the treated and untreated areas at different magnifications, c – indication of the areas of study of the composition

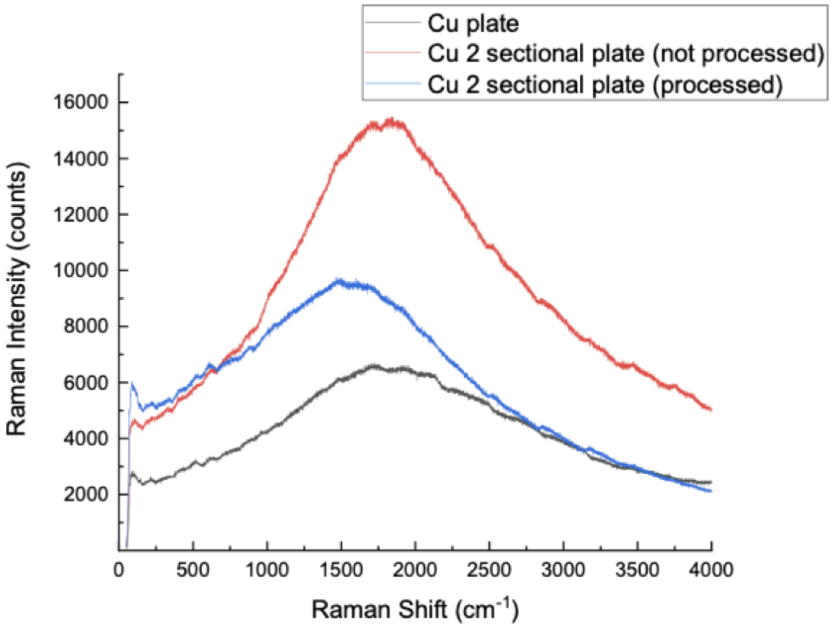

**Fig. 3.** Raman spectra of copper sample

Figure 4 shows the surface of a nickel electrode at the border of the treated and untreated areas at different magnifications. The untreated area is a smooth nickel surface. As a result of exposure to laser radiation, a significant restructuring of the surface occurs. The lines of the laser beam 50 µm wide are clearly visible on it. The transition region 10 µm wide corresponds to the main part of the Gaussian of the intensity distribution of the falling part of the Gaussian of the intensity distribution of the laser beam.

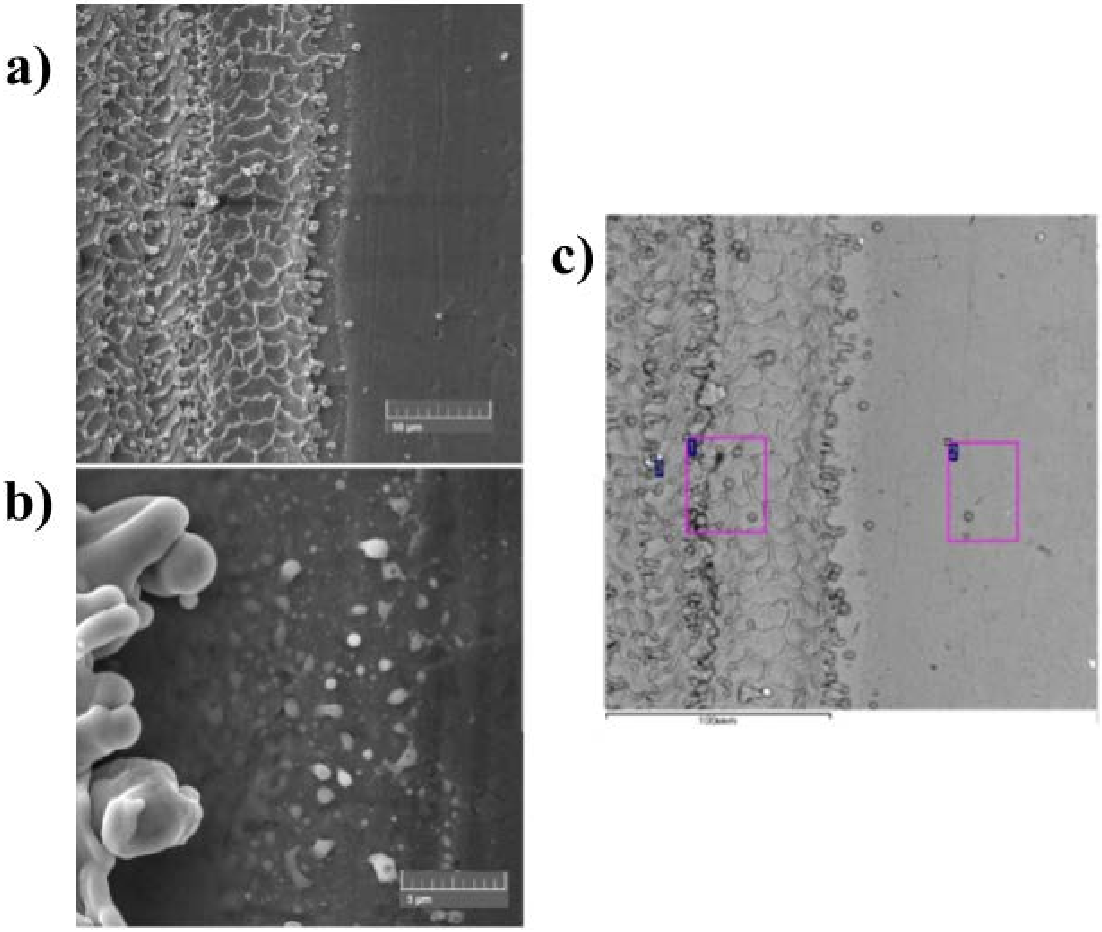

**Fig. 4.** (a,b) SEM images of the nickel electrode surface at the border of the treated and untreated areas at different magnifications, c – indication of the areas of study of the composition

Table 3. Results of energy dispersive surface studies. All results are in weight percent

| Point | O | Al | Ni |
|---|---|---|---|
| 1 | 3.40 | 0.72 | 95.88 |
| 2 | 4.04 |  | 95.96 |

EDX indicates (Table 3) that as a result of laser treatment, the composition of the surface does not change significantly: in both cases, it is composed of Ni 99.92 ± 0.04. That is, when the surface is treated with a laser in an uncontrolled medium, the surface is not oxidized, which correlates with the results of Raman spectroscopy (Fig. 5).

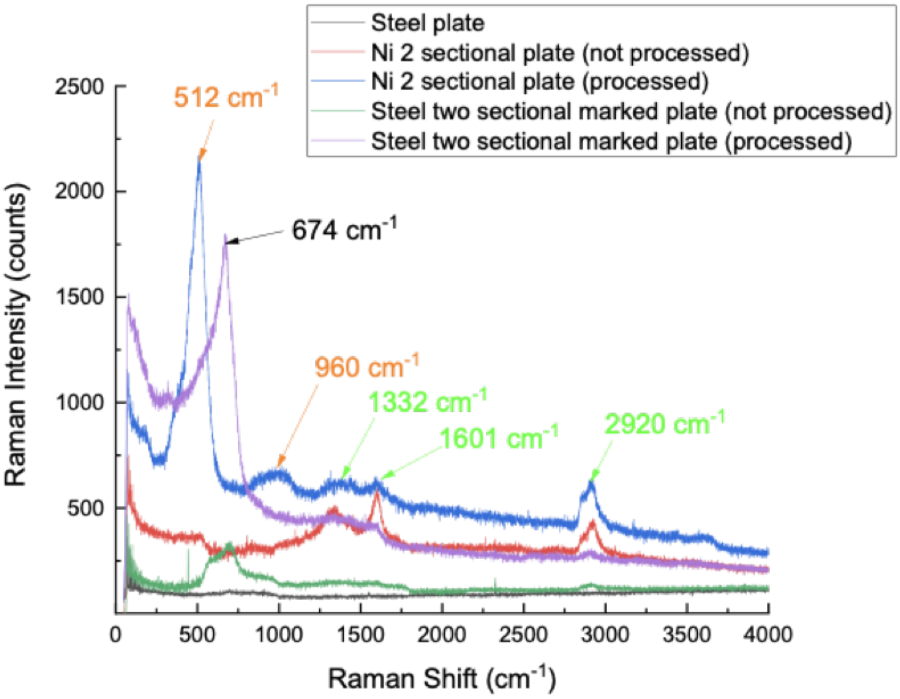

**Fig. 5.** Raman spectra of nickel and steel samples

The peaks in Fig. 5 at 512 cm$^{-1}$ (LO) and 960 cm$^{-1}$ (2LO) correspond to NiO. In the red spectrum obtained from the untreated half of the sample, these peaks are absent, which indicates the absence of oxide. The green peaks in Fig. 5, according to their nature, have nothing to do with Ni or NiO. They correlate well with the spectra of amorphous carbon films: 1332 cm$^{-1}$ and 1601 cm$^{-1}$ correspond to D and G modes, respectively. The presence of the G-mode confirms the presence of a graphite phase with a good degree of ordering, but a shift of its peak (1575 cm$^{-1}$ according to [16]) towards large values indicates an increase in disorder in the structure. The D-mode corresponds to amorphous carbon. The peak corresponding to 2920 cm$^{-1}$ can be attributed to the combination of these two modes (D + G). Comparing the obtained spectrum with the spectra of a graphene monolayer [17] and an amorphous carbon film [18], it can be argued that there is no graphene on the Ni surface with a high degree of probability, or there is very little graphene phase because there is no 2D mode typical for graphene, but there is D + G, which is not typical for amorphous carbon.

Laser treatment of steel (Fig. 6) also results in a pattern formation, in which the lines of the laser beam 50 μm wide are clearly visible (similar to nickel). Here, significant melting of the surface with the formation of a developed structure is also observed. In addition, the image of the untreated part of the sample shows the presence of a large number of spherical particles, probably due to the formation of metal droplets under the action of laser radiation.

Table 4. Results of energy dispersive surface studies. All results are in weight percent

| Point | O | Si | Cr | Mn | Fe | Ni |
|---|---|---|---|---|---|---|
| 1 | 2.38 | 0.46 | 19.14 | 1.23 | 69.25 | 7.53 |
| 2 | 38.16 | 0.30 | 12.62 | 0.48 | 43.80 | 4.64 |

EDX (Table 4) indicates that the surface is slightly oxidized, except for the formation of spherical particles: they are composed essentially of the oxide phase. Similar to the previous one, in the treated area, spherical particles are observed, which are an oxide phase formed during the rapid oxidation of droplets of the material melt. That is, when the surface is treated with a laser in air, the metal drops knocked out by the laser beam are oxidized, that is, a parallel process of material consumption occurs, which reduces the efficiency of obtaining a developed surface.

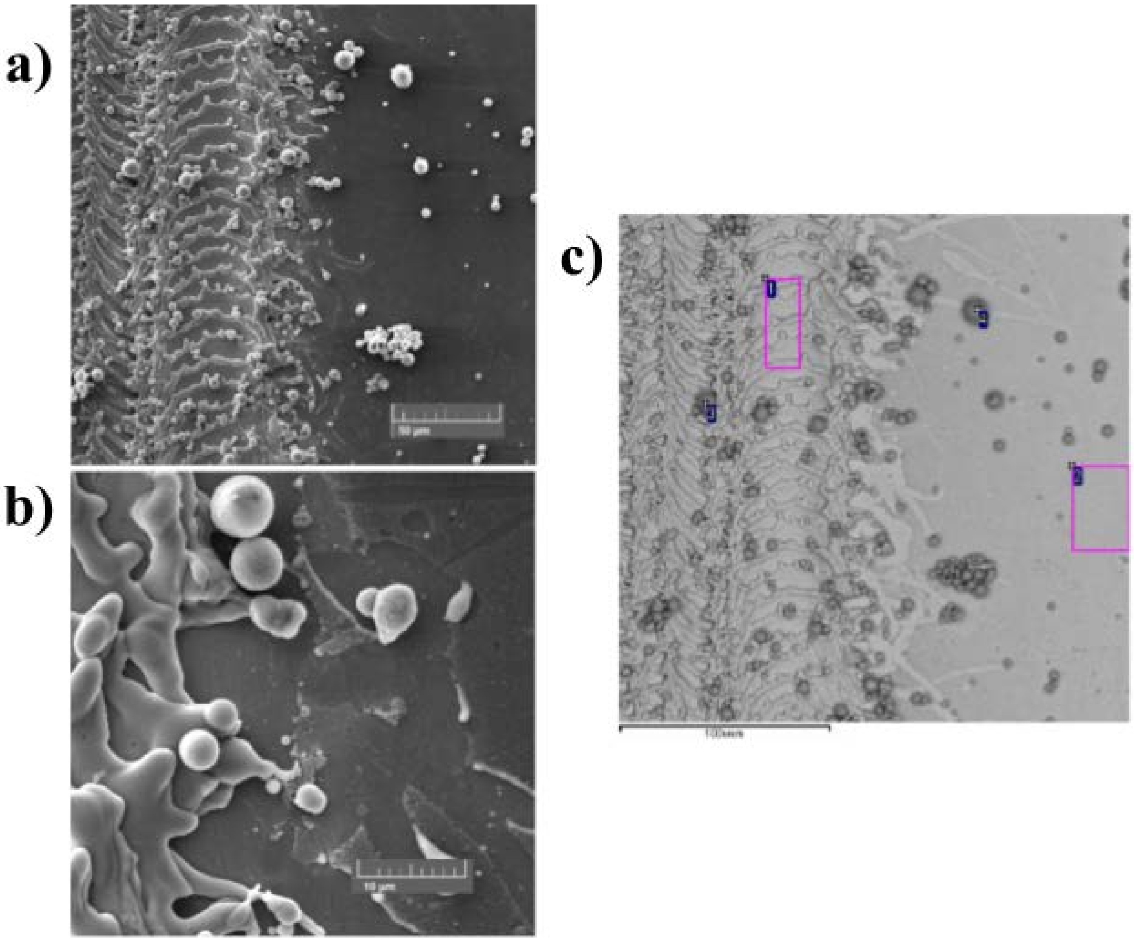

**Fig. 6.** (a, b) SEM images of the steel electrode surface at the border of the treated and untreated areas at different magnifications, c – indication of the areas of study of the composition

In the case of a steel electrode, Raman spectroscopy turned out to be less informative (Fig. 5). The spectrum of black color, obtained on an untreated steel plate, demonstrates the absence of any response, this form of the spectrum is typical for this material [19]. Violet and green spectra of the processed sample also contain peaks associated with carbon (green peaks), but of much lower intensity, which may indicate a smaller thickness of the grown layer of the same carbon. An exception is a peak at 674 $cm^{-1}$, which may correspond to iron oxide $Fe_3O_4$ [20].

Thus, laser-driven alteration on copper, nickel, and steel occurs in different ways, due to differences in the thermal conductivity of materials. The results indicate the fundamental suitability of the method of laser-driven alteration of various metal foils for the formation of electrodes for the electrochemical determination of glucose in solution since they make it possible to quickly and reproducibly obtain a developed metal surface. Of the materials considered, the nickel surface treatment is the most promising , since it is not accompanied by the formation of additional parasitic phases.

To study the sensitivity of the formed electrodes to the presence and concentration of glucose in the solution, a technique that allows electrochemically investigating the ongoing processes was developed. At the first stage, the behavior of nickel foil in a 0.1 M NaOH solution was under investigation. It was found that in the case of using an untreated nickel substrate as a working electrode, the characteristic peaks of the Ni(III)/Ni(II) transition at about 0.4 V [21] are not observed. Additional electrochemical treatment (cathodic and anodic), etching, and mechanical activation of the surface of the initial foil also did not lead to the appearance of a corresponding peak in CV. In the case of using a preliminarily laser-altered nickel foil as a working electrode (Fig. 7), characteristic peaks of the Ni(III)/Ni(II) transition are observed for all rates of potential change. The formation of hydroxide on the treated surface most likely occurs during contact of the material with the solution.

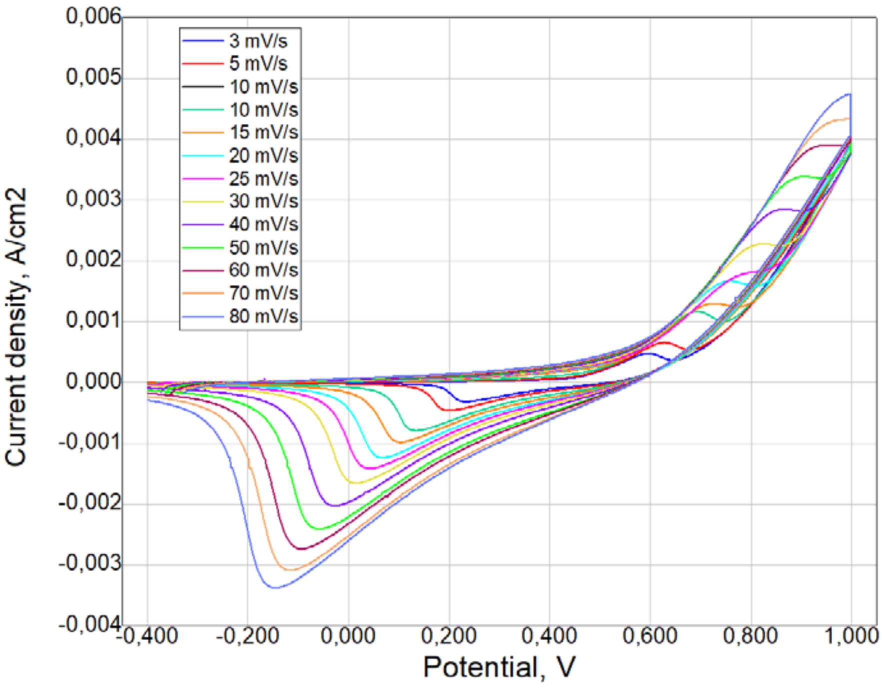

**Fig. 7.** Cyclic voltammograms of laser-altered nickel foil

In the case of adding 0.1 mM glucose to the working solution, a peak of about 0.4 V is also observed, the intensity of which is higher than for the case of CV without glucose (Fig. 8a). This result unambiguously indicates that electrodes for the electrochemical determination of glucose in the solution can be obtained by the method of laser-driven alteration of nickel foils. The areas of linear dependence of the current on the sweep speed will allow in the future to select the most convenient areas of the device operation parameters (Fig. 8b). The increase in the current of characteristic peaks on CV can be associated with surface glucose oxidation to form gluconate ion and hydronium ion [22-25].

During potentiostatic measurements (Fig. 9): 0-30 sec – the electrochemical circuit is open, the current is 0; at 30 seconds, a potential is applied and a current is recorded, when the circuit is closed, a sharp increase in current occurs; the system is turned off for 150 seconds. It can be seen that the introduction of glucose immediately provokes an increase in the current. The calculated values of the sensitivity are higher than 10 μA/(mM·cm$^2$), the detection limit is not less than 5 μM, the signal-to-noise ratio is 5.

Thus, the proposed technique of laser-driven alteration of nickel foils for electrochemical determination of glucose in solution electrode formation makes it possible to form active parts of sensors that are sensitive to glucose in the concentration range from 100 to 1500 μM with sufficient sensitivity and reproducibility.

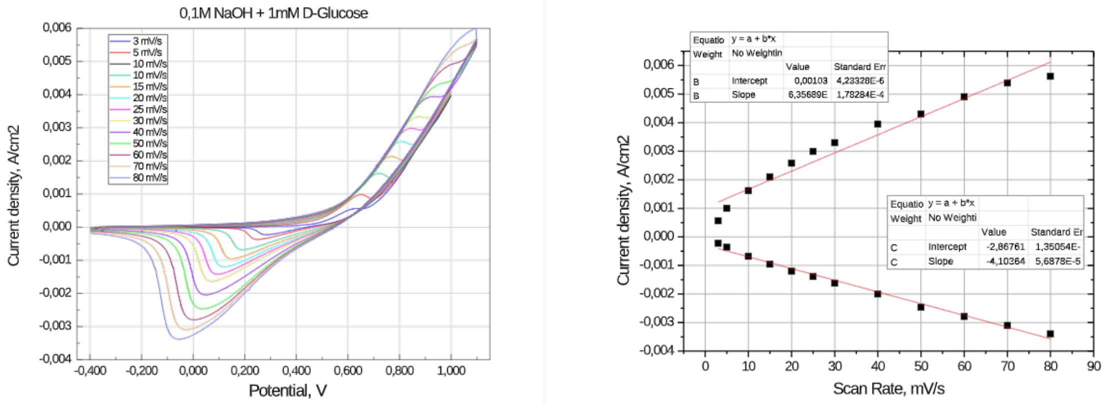

(a) (b)

**Fig. 8.** (a) Cyclic voltammograms of activated nickel foil and (b) currents of the anode and cathode legs at different rates of change in the scan potential

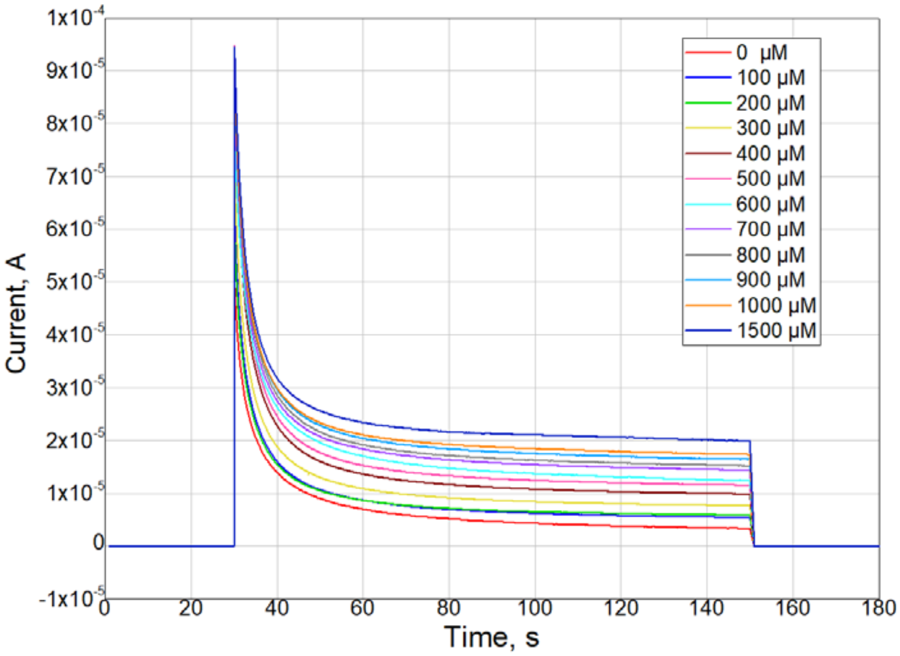

**Fig. 9.** Results of potentiostatic measurements (current response) at different glucose concentrations

## 4. Conclusions

The manufactured active layer of the sensor made of nickel oxide allows the amperometric determination of glucose in the concentration range from 10 µM to 1.5 mM, the sensitivity is higher than 10 µA/(mM·cm$^2$), the detection limit is not less than 5 µM, the signal-to-noise ratio is 5.

The method of laser-driven modification of a metal surface can be used to manufacture active elements of a non-enzymatic glucose sensor. The ease of scaling the results is due to the ease of observing the geometry of the device and the absence of complex technological operations during its manufacture. The next stage in the development of the prototype will be the development of a test system and a system for removing and processing signals.

## References

[1] Jeevanandham G, Jerome R, Murugan ., Preethika ., Vediappan ., Sundramoorthy AK. Nickel oxide decorated MoS 2 nanosheet-based non-enzymatic sensor for the selective detection of glucose. *RSC Advances.* 2020;10(2): 643-654.

[2] Juska VB, Pemble ME. A critical review of electrochemical glucose sensing: evolution of biosensor platforms based on advanced nanosystems. *Sensors.* 2020;20(21): 6013.

[3] Singer N, Pillai RG, Johnson AID, Harris KD, Jemere AB. Nanostructured nickel oxide electrodes for non-enzymatic electrochemical glucose sensing. *Microchimica Acta.* 2020;187(4): 1-10.

[4] Visotskaya AV, Kosenko NM. *Non-invasive blood glucose sensing*. 2020. (In Russian).

[5] Choi T, Kim SH, Lee CW, Kim H, Choi SK, Kim SH, Kim E, Park J, Kim H. Synthesis of carbon nanotube–nickel nanocomposites using atomic layer deposition for high-performance non-enzymatic glucose sensing. *Biosensors and Bioelectronics.* 2015;63: 325-330.

[6] Guo C, Wang Y, Zhao Y, Xu C. Non-enzymatic glucose sensor based on three dimensional nickel oxide for enhanced sensitivity. *Analytical Methods.* 2013; 5(7): 1644-1647.

[7] Wang G, He X, Wang L, Gu A, Huang Y, Fang B, Geng B, Zhang X. Non-enzymatic electrochemical sensing of glucose. *Microchimica Acta.* 2013;180(3-4): 161-186.

[8] Niu X, Lan M, Zhao H, Chen C. Highly sensitive and selective nonenzymatic detection of glucose using three-dimensional porous nickel nanostructures. *Analytical Chemistry.* 2013; 85(7): 3561-3569.

[9] Zahmouli N, Marini S, Guediri M, Ben Mansour N, Hjiri M, El Mir L, Espro C, Neri G, Leonardi SG. Nanostructured nickel on porous carbon-silica matrix as an efficient electrocatalytic material for a non-enzymatic glucose sensor. *Chemosensors.* 2018;6(4): 54.

[10] Paulose R, Mohan R, Parihar V. Nanostructured nickel oxide and its electrochemical behavior. *A brief review*. *Nano-Structures & Nano-Objects.* 2017;11: 102-111.

[11] Bonomo M. Synthesis and characterization of NiO nanostructures: a review. *Journal of Nanoparticle Research.* 2018;20(8): 1-26.

[12] Marini S, Ben Mansour N, Hjiri M, Dhahri R, El Mir L, Espro C, Bonavita A, Galvagno S, Neri G, Leonardi SG. Non-enzymatic G
Composite. *Electroanalysis.* 2018;30(4): 727-733.

[13] Thoufeeq S, Rastogi PK, Sreekanth N, Anantharaman MMRI, Narayanan TN. Nickel-reduced graphene oxide composite foams for electrochemical oxidation processes: towards biomolecule sensing. *MRS Communications.* 2018;8(3): 695-702.

[14] Zolotariov VM, Morozov VN. *Optical constants of natural and technical environments. Handbook.* Leningrad: Khimia; 1984. (In Russian).

[15] Gergely A. A review on corrosion protection with single-layer, multilayer, and composites of graphene. *Corrosion Reviews.* 2018;36(2): 155-225.

[16] Kassab LRP, Santos AD, Pillis MF. Evaluation of carbon thin films using Raman spectroscopy. *Materials Research.* 2018;21(4): e20170787.

[17] Barron AR. *Physical methods in chemistry and nano science*. 2015.

[18] Dychalska A, Popielarski P, Frankówet W, Fabisiak K, Paprocki K, Szybowicz M. Study of CVD diamond layers with amorphous carbon admixture by Raman scattering spectroscopy. *Mater. Sci.-Pol.* 2015;33(4): 799-805.

[19] Valeev RG, Stashkova VV, Chukavin AI, Volkov VA, Alalykin AS, Syugaev V, Beltiukov AN, Gil’mutdinov FZ, Kriventsov VV, Mezentsev NA. Ni nanostructures in porous anodic alumina matrices: structure and cathodic properties in hydrogen release reactions. *Physics Procedia.* 2016;84: 407-414.

[20] Hai NH, Phu ND, Luong NH, Chau N, Chinh HD, Hoang LH, Leslie-Pelecky DL. Mechanism for sustainable magnetic nanoparticles under ambient conditions. *Journal of the Korean Physical Society*. 2008;52(5): 1327-1331.

[21] Kondrateva AS, Bespalova P, Baryshev GK, Mishin M.. Electrochromic Properties of NiO Thin Coatings. *Key Engineering Materials*. 2019;822: 781-786.

[22] Song YY, Zhang D, Gao W, Xia XH. Nonenzymatic glucose detection by using a three-dimensionally ordered, macroporous platinum template. *Chemistry A European Journal.* 2005;11(7): 2177-2182.

[23] Kun T, Baskaran K, Tiwari A. Nonenzymatic glucose sensing using metal oxides–comparison of CuO, Co3O4, and NiO. *Vacuum.* 2018;155: 696-701.

[24] Yang B, Qiao J, Yu Y, Yuan L, Hu X. The simple-preparation of Cu–Ni/CuO–NiO using solution plasma for application in a glucose enzyme-free sensor. *New Journal of Chemistry.* 2020;44(26): 10806-10812.

[25] Lipińska W, Ryl J, Slepski P, Siuzdak K, Grochowska K. Exploring multi-step glucose oxidation kinetics at GOx-functionalized nanotextured gold surfaces with differential impedimetric technique. *Measurement.* 2021;174: 109015.

## THE AUTHORS

**Kondrateva A.S.**
e-mail: a.s.kondrateva@yandex.ru
ORCID: 0000-0003-3915-9329

**Babuk V.E.**
e-mail: vladislavbabyuk@gmail.com
ORCID: 0000-0002-4448-4567

**Strekalovskaya D.A.**
e-mail: darya.strek@gmail.com
ORCID: 0000-0001-9965-7966

**Filatov L.A.**
e-mail: phylatov@yandex.ru
ORCID: 0000-0001-6446-5059

**Gabdullin P.G.**
e-mail: gabdullin_pg@spbstu.ru
ORCID: 0000-0002-2519-2577

**Kvashenkina O.E.**
e-mail: kvol.spbspu@gmail.com
ORCID: 0000-0002-7546-8359

**Prokopenko Y.Y.**
e-mail: lekanmoon@gmail.com
ORCID: 0000-0002-3282-9951

**Gruzdev A.S.**
e-mail: gruzdev-spb@yandex.ru

ORCID: 0000-0001-5168-3786

**Petruhno K.A.**
e-mail: k.a.petroukhno@gmail.com
ORCID: 0000-0001-7424-3345

**Kuznetsov A.S.**
e-mail: alkuznetsov1998@gmail.com
ORCID: 0000-0001-7143-6686